

## EVAPORATIVE COOLING SYSTEMS APPLICATIONS IN BRASÍLIA: CASE STUDIES

Wagner Pereira de Castro  
wagnerpc@pop.com.br

João Manoel Dias Pimenta  
pimenta@enm.unb.br

### Resumo

Resultados de um estudo de engenharia sobre a aplicação de sistema de resfriamento evaporativo, para geração de energia em pequena escala e climatização de ambientes, são apresentados nesse artigo. Um primeiro caso de estudo considera a análise do potencial de um painel evaporativo direto, acoplado a um ciclo de microturbina a gás existente. Um estudo paramétrico dos efeitos do resfriamento evaporativo do ar sobre variáveis com eficiência e potência gerada, é investigado, assim como o desempenho da microturbina ao longo do ano teste de referência (TRY) em Brasília. O segundo caso de estudo está relacionado à aplicação de um sistema de resfriamento evaporativo, para conforto térmico do Centro Comunitário da Universidade de Brasília. A determinação do sistema de resfriamento foi baseada na máxima carga de resfriamento calculada para um dia de verão, no ano teste de referência em Brasília. Resultados diversos são apresentados a respeito dos casos de estudo avaliados.

*Palavras-chave:* resfriamento evaporativo, conforto térmico, geração de energia, simulação.

### Abstract

Theoretical results from an engineering study concerning the application of evaporative cooling systems for small-scale power generation and ambient thermal comfort are presented in this paper. A first case study considers an analysis on the potential of a direct evaporative media coupled to an existing gas microturbine cycle. A parametric study of the effects of the air combustion evaporative cooling about variables as cycle efficiency and output power, is investigated, so the microturbine performance along the test reference year (TRY) in Brasilia. The second case study is related to the application of an evaporative cooling system for space conditioning of the Community Center of the University of Brasilia. The determination of the evaporative cooling system was realized based in the maxim thermal load calculated for a day summer in the Test Reference Year in Brasilia. Results are presented concerning that two case studies.

*Keywords:* evaporative cooling, thermal comfort, power generation, simulation.

## 1 Introdução

Evaporative cooling is a natural process involving air temperature reduction and humidity increase thanks to simultaneous heat and mass transfer between air and water. Recently evaporative cooling systems have been used in several engineering applications such as: human thermal comfort in large spaces, industrial humidification, supply air cooling for gas turbines, poultry livestock buildings etc. Specifically in the field of power generation, previous studies have shown the advantages of the use of evaporative panels for supply air conditioning in gas turbines (GUIMARÃES 2000, BASSILY 2001), which is mainly based on the fact that, at lower temperatures, air density is higher allowing to promote a greater mass flow rate introduction to

the combustion chamber. This allows increasing annual power generation in 2 to 4% in hot and dry climates (DE LUCIA, LANFRANCHI, and BOGGIO, 1995; DE LUCIA et al., 1997). However, studies applied to small scale distributed generation, as for instance in microturbine based cycles still rare in the literature.

On the other hand, evaporative cooling applied to ambient conditioning has motivated several studies. Evaporative cooling has been adopted with success in large spaces air conditioning with high cooling loads, such as in industrial and commercial application. Such conditions impose economic constraints to the use of conventional air conditioning systems, making evaporative cooling an adequate choice. Other advantages in evaporative systems use for ambient comfort are: it has very low energy consumption when compared to conventional conditioning systems; installation and maintenance costs are lower; evaporative cooling system operation is simpler. installation and integration with existing conditioning systems can be easily made (CAMARGO and EBINUMA, 2001). Besides, since evaporative cooling systems uses integral fresh air (no recirculation) problems related with fungus and bacteria will be reduced.

## 2 Direct Evaporative Cooling Process

There are two schemes of implementation of the evaporative cooling process: direct and indirect. For the direct scheme. Fig. 1a, outside air is cooled and humidified by direct contact with a wet surface (an evaporative panel generally made in cellulose), or with a water spray. This causes simultaneous water mass transfer (to the air flow, increasing its water content) and air wet bulb temperature reduction. If heat loss to surroundings are neglected the process is adiabatic, i.e., some sensible heat is transferred from air but an equal amount of latent heat is transferred to it. On a psychometric chart, the process follows a constant enthalpy line, Fig. 1b, but, since the difference between constant wet bulb temperature and constant enthalpy lines are negligible, the direct evaporative cooling process can be assumed as being a constant wet bulb temperature one.

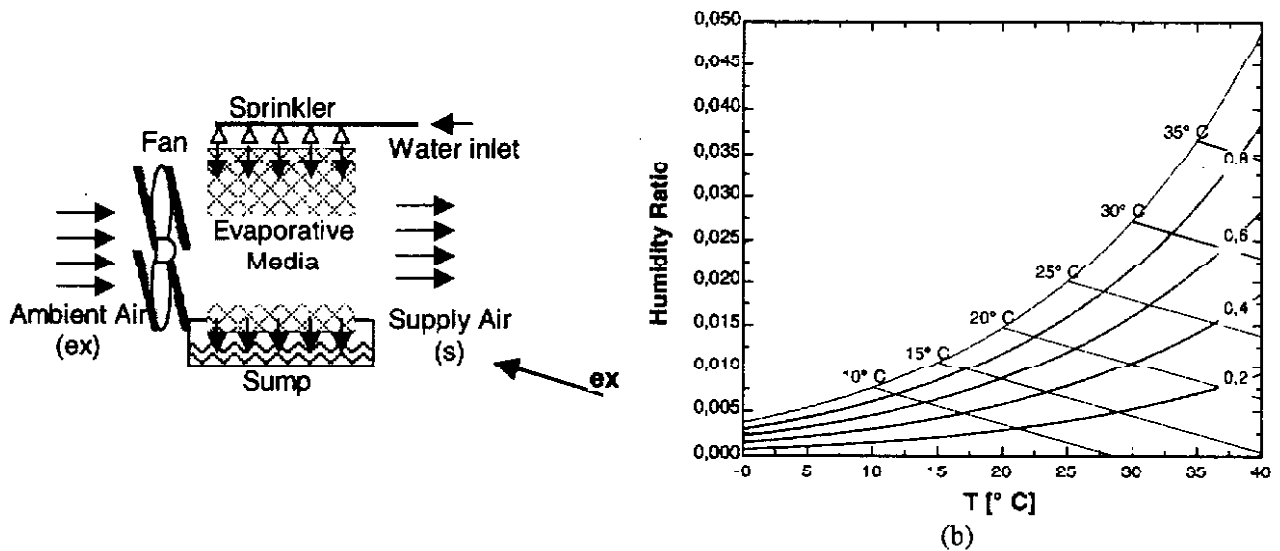


Figure 1 - Schematic representation of a direct evaporative cooling system (a) and its process representation in the psychometric chart (b).

An important parameter in the characterization of evaporative cooling equipment is related to its effectiveness  $\epsilon_d$ , which is defined as the ratio between actual ( $T_s - T_{ex}$ ) and theoretical ( $T_{ex} - T_{bu}$ ) air temperature decrease across the evaporative media, as given by the following equation,

$$\epsilon_d = \frac{T_s - T_{ex}}{T_{ex} - T_{bu}} \quad (1)$$

which allow to calculate outside air a temperature ( $T_s$ ) from a direct evaporative system like that from Fig. 1a, by,

$$T_s = T_{ex} - \epsilon_d \cdot (T_{ex} - T_{bu}) \quad (2)$$

In ideal theoretical conditions, air temperature drop ( $T_{ex}-T_{bu}$ ) refers to an ideal condition where air outside dry bulb temperature ( $T_{ex}$ ) equals its entering wet bulb temperature ( $T_{bu}$ ) at panel inlet conditions.

Once the air inlet velocity and evaporative panel thickness are specified, it is possible to obtain the nominal effectiveness of the panel from performance curves such as those shown at Fig. 2.

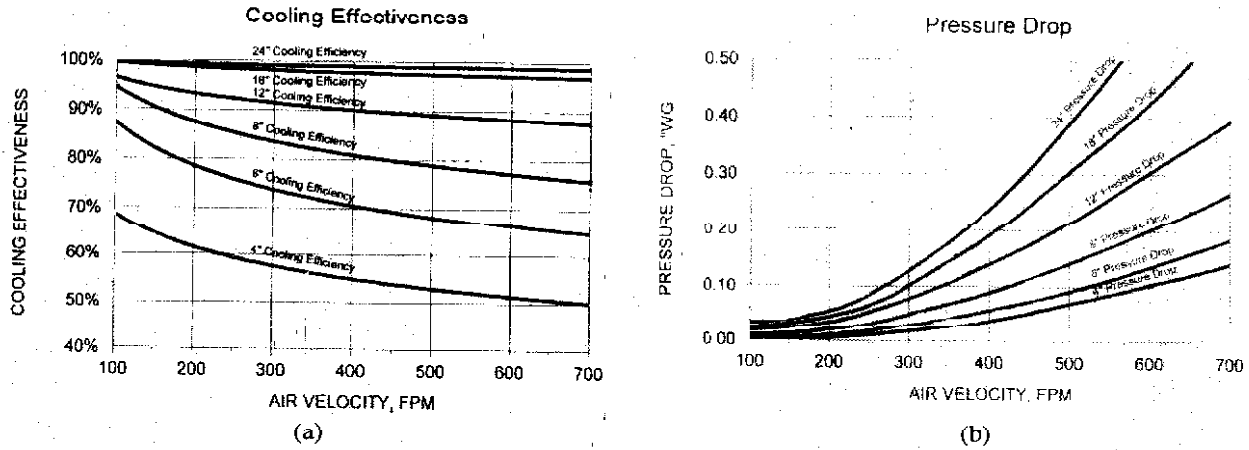


Figure 2 - Characteristic curves for effectiveness (a) and air pressure drop (b) in a commercial evaporative panel for different panel thickness and air velocities (from Munters™).

Since a constant wet bulb temperature process is assumed, air thermodynamic state is determined, while air mass flow rate ( $\dot{m}_{ar}$ ) through the panel will depend on the thermal load as given by,

$$\dot{m}_{ar} = \frac{\dot{Q}_{latente} + \dot{Q}_{sensível}}{c_{pu} \cdot (T_r - T_s)} \tag{3}$$

where  $T_r$  is the dry bulb temperature of air in the zone and,  $c_{pu}$  is the specific heat of the air  $\dot{Q}_{latente}$  and  $\dot{Q}_{sensível}$  being the sensible and latent heat transfer rates from the ambient, respect. In ambient air conditioning values from 3,9 up to 5 °C are considered acceptable for the temperature difference between air in the space and air delivered at the cooling panel outlet (WATT, 1984). At his turn, air pressure at the panel outlet ( $p_s$ ) is given by,

$$p_s = p_{ex} - \Delta p \tag{4}$$

where  $p_{ex}$  is the air pressure at the inlet and  $\Delta p$  is the pressure drop in the evaporative media. As is assumed a constant air wet bulb temperature at the evaporative cooling process, the air state at the outlet is characterized.

For the absolute humidity in the conditioned space ( $W_r$ ), we verify that it depends on the air conditions delivered to the space as well as the latent load. A good estimation on this is given by (JOURDI and MEHDI, 2000).

$$W_r = W_s + \frac{\dot{Q}_{latente}}{\dot{m}_{ar} h_{lv}} \tag{5}$$

where  $W_s$  is the air absolute humidity at the evaporative panel outlet and  $h_{lv}$  is the latent heat of vaporization for water assumed constant and equal to 2454 kJ/kg.

### 3 Case Studies – Description and Methodology

#### 3.1 Case 1 - Air Evaporative Cooling for Microturbine Based Power Cycle

Gas microturbines are compact power generation devices, similar to conventional gas turbines which are being considered more and more as an alternative solution for electric power distributed generation.

In this first case study a theoretical analysis is carried out on the feasibility application of evaporative direct contact panels for air conditioning at microturbine compressor supply. For such a purpose an actual microturbine designed, built and presently under experimental testing at the Departamento de Engenharia Mecânica/ UnB was considered. The experimental apparatus consists on a centrifugal turbo-compressor unit and a combustion chamber designed to stoichiometric burning of an amount of 24% do inlet air (SANTOS, 2002). The analysis has considered a single operation point for the power cycle, using methane ( $\text{CH}_4$ ) fuel. On the basis of experimental data carried out previously in the microturbina test bench (SANTOS, 2002), a constant fuel mass flow rate of 0.0043kg/s was taken using a pressure ratio of 1,6 and an isentropic efficiency of 75% and 85% for the compressor and microturbine, respect.

Since the panel should be mounted at the compressor inlet, its selection is based on the air velocity at supply conditions. For operation according to ISO Standard conditions of local air temperature and relative humidity of 295.15 K and 60% respect, the inlet velocity was calculated as being about 0,780 m/s (155 ft/min). For such velocity, if a evaporative panel of 12 inches of thickness is choose, the characteristic curves of Fig. 2 allow to obtain a nominal effectiveness of 95 % and a pressure drop of 40Pa for the selected evaporative panel.

Figure 3 shows a schematic view of the system in study and a representation of the whole thermodynamics process. Basically the system consists on a classical Brayton open cycle with a evaporative cooling panel mounted at the compressor air supply, which is hereafter identified by EGMTC cycle. For purpose of comparisons, we will also consider the classical Brayton open cycle without the evaporative cooling panel (hereafter identified by GMTC cycle). During the EGMTC cycle, ambient air is cooled and humidified before it enters the compressor (C) at point 1, where air temperature will be closer the ambient wet bulb temperature. At compressor exhaust (point 2) air is supplied to the combustion chamber (CC), where fuel and air are mixed and burned resulting in combustion products at point 3 which are finally expanded in a gas microturbine (GMT).

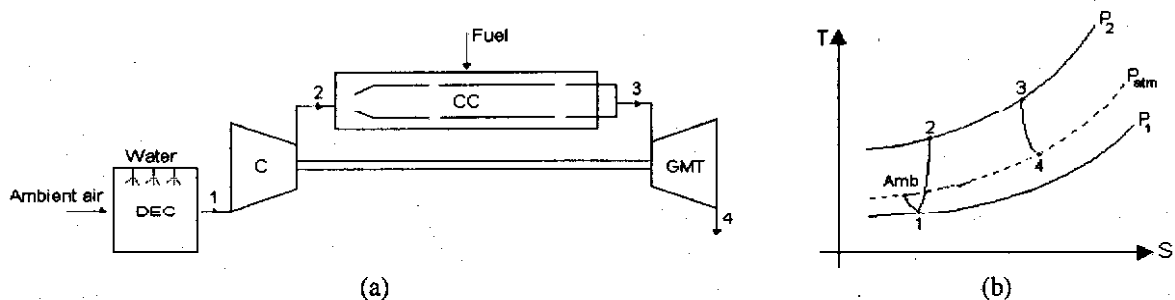


**Figura 3** - Microturbine based open Brayton cycle with evaporative air cooling at compressor inlet. (a) Schematic view of the system. (b) Temperature-entropy representation for the cycle.

On the basis of the data described above, a parametric analysis on the effects of evaporative cooling on the Brayton cycle is carried out. Such analysis takes into account the influence of evaporative cooling on cycle efficiency and net power generation under different operating conditions for both GMTC and EGMTC cycles. The systems are then simulated for climatic data for a whole Test Reference Year (TRY) for the city of Brasília, in order to verify the feasibility of application of evaporative cooling panels to the proposed microturbine cycle.

#### 3.2 Case 2 – Cooling Load in the Community Center of the University of Brasília

The Community Center of the Brasília University (UnB) is a building for large events, like shows conferences, etc. It basically consists in a large elliptic tent with approximately 40m x 80m, composed by a steel cables frame structure supporting a synthetic white canvas with 0,88 mm of thickness, which is stretched to obtain a hyperbolic-parabolic contour shape thanks to six main posts, as shown in Fig. 4. The canvas is built in high strength polyester with a surface coating in polyvinylidene

ruoride (PVDF) resin having a total reflectivity of 70% and a total solar absorptivity of 15%. The net area for occupants is about 37m x 74m, which allow accommodating an average of 3000 seated occupants. However the Community Center presents some thermal overload problems and inadequate ventilation during periods of full occupation. Because the ambient is fully open (which favors a full air renovation) and because it is located in Brasília (which has high temperature difference between dry and wet air temperatures during the whole year), the use of an evaporative system is strongly recommended. With these considerations in mind, this case study considers the application of an evaporative cooling system for thermal comfort purposes (25 °C dry bulb temperature 60% relative humidity) at the Community Center of the (UnB).

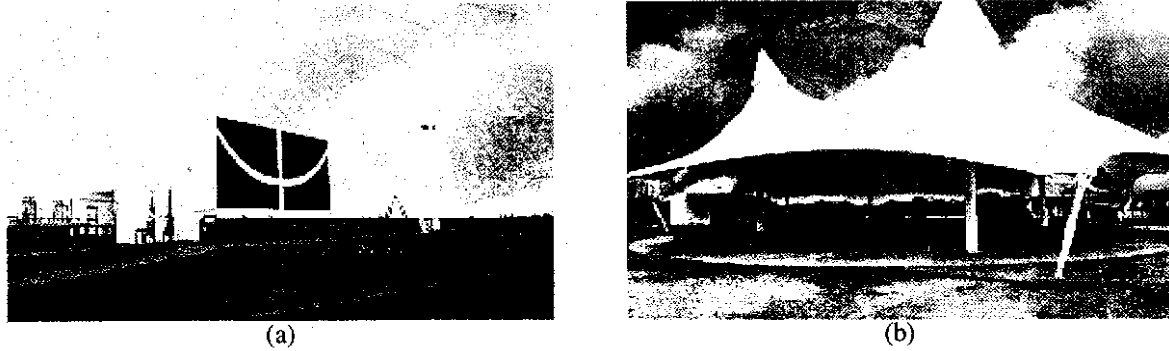


Figure 4 - UnB Community Center. (a) Internal view of the Center. (b) External partial view of the canvas surface.

From an energy balance for the canvas frame, the hourly cooling load for the whole tent is calculated taking into account factors like constructive details, occupants and local weather data (based on Test Reference Year for Brasília). This case study gives special focus to the canvas roof analysis due to its peculiar geometry and large surface area exposed to solar irradiation. A direct water spraying evaporative cooling system is then designed on the basis of a peak cooling load during the period of analysis considered. The design procedure starts from the selections of the spray nozzles to be used, then, considering an equal height of 8 meters from floor, sprays having an orifice diameter of 0.2 mm with nominal flow rate of 4 liters/h each (Prime Tech™) and producing water drops with a diameter of 10 µm were selected. Next were defined the number of spray nozzles, as well as the size of the pump for the spray network.

#### 4 Case Studies – Model and Simulation

##### 4.1 Case 1 - Air Evaporative Cooling for Microturbine Based Power Cycle

From the parameters considered for the system under study, as well as from TRY weather conditions defined, it was possible to simulate the microturbine power cycle with evaporative cooling at compressor inlet. The modeling considers a Brayton open cycle in steady state with negligible changes in kinetic and potential energy. The compressor, combustion chamber and microturbine are all considered as adiabatic with negligible pressure drops. Air and flue gases absolute humidity are taken as having the same value and atmospheric pressure is assumed at the microturbine exhaust port.

With these considerations, the application of a direct evaporative cooling system will reduce compressor supply temperature ( $T_1$ ) to a value determined from Eq. (2). After adiabatic compression (with a pressure ratio  $r$ , and isentropic efficiency  $\eta_c$ ) from pressure  $p_1$ , air reaches a temperature  $T_2$  at the compressor exhaust, calculated by (COHEN, ROGERS and SARAVANAMUTTOO, 1996),

$$T_2 = T_1 \cdot \left[ 1 + \frac{1}{\eta_c} \cdot \left( r^{\frac{\gamma_c - 1}{\gamma_c}} - 1 \right) \right] \quad (6)$$

where  $\gamma_c$  is the specific heat ratio at constant pressure and constant volume conditions. Compressor exhaust pressure ( $p_2$ ) is calculated from the inlet pressure ( $p_1$ ) and pressure ratio. It is also assumed that air absolute humidity remains constant during compression. Once the compressor inlet and outlet conditions are known it is possible to calculate the compression power ( $\dot{W}_c$ ), from a energy balance for the compressor as follows,

$$\dot{W}_c = \dot{m}_{ar} \cdot (h_2 - h_1) \quad (7)$$

where  $h_1$  and  $h_2$  are the air enthalpies at compressor supply and exhaust respectively.

In the combustion chamber about 76% of the total air flow rate is by-passed and will not take part in the combustion reaction, while the other 24 % of air flow is introduced in the burning chamber trough its dilution holes. After the combustion both streams of combustion products and by-passed air are mixed at combustion chamber outlet as shown at Fig. 5a.

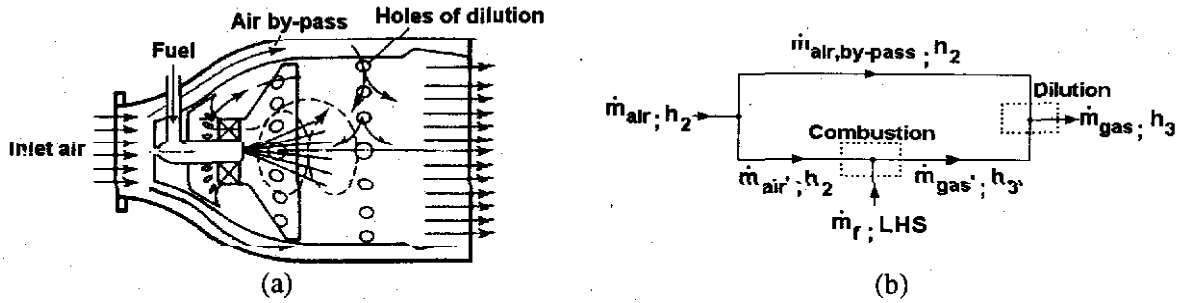


**Figure 5** - Modeling for the microturbine cycle combustion chamber. (a) Basic construction of the combustion chamber (COHEN, ROGERS and SARAVANAMUTTOO, 1996) and (b) energy flow diagram for the combustion process.

Figure 5b represents the simplified modeling approach adopted for the analysis of the combustion chamber. Neglecting heat transfer from the internal chamber surface to the by-passed air stream, the energy and mass balances allow to obtain the specific enthalpy of flue gases delivered for expansion at the microturbine ( $h_3$ ) as,

$$h_3 \cdot \dot{m}_{gas} = \dot{m}_{ar} \cdot h_2 + \dot{m}_f \cdot LHS \quad (8)$$

where  $\dot{m}_{gas}$  is the flue gases mass flow rate resulting from the mixing between combustion products and by-passed air, while  $\dot{m}_f$  and  $LHS$  are the fuel ( $CH_4$ ) mass flow rate and low heating value (taken as 49962.1 kJ/kg for methane) respectively. The thermodynamic state of flue gases at microturbine inlet is then determined and it is now possible to calculate the temperature at the microturbine exhaust ( $T_4$ ) by means of (COHEN, ROGERS and SARAVANAMUTTOO, 1996),

$$T_4 = T_3 \cdot \left[ 1 - \eta_t \cdot \left[ 1 - \left( \frac{1}{p_3/p_4} \right)^{(\gamma_t-1)/\gamma_t} \right] \right] \quad (9)$$

where  $\gamma_t$  is the constant pressure, constant volume specific heats ratio of the gases at the microturbine exhaust and  $\eta_t$  represents the isentropic efficiency of the microturbine. Now the gross power generation at the turbine as a result of the expansion process can be calculated simply by means of,

$$\dot{W}_t = \dot{m}_{gas} \cdot (h_3 - h_4) \quad (10)$$

where  $h_3$  e  $h_4$  are the specific enthalpies of flue gases at the microturbine inlet and outlet respect.

The net power production from the cycle is then obtained from the difference between compressor power consumption and turbine gross power production, allowing to define an overall cycle efficiency ( $\eta$ ) given by

$$\eta = (\dot{W}_t - \dot{W}_c) / \dot{m}_f \cdot LHS \quad (11)$$

while it is also possible to obtain the specific fuel consumption (SFC) by means of,

$$SFC = \dot{m}_f / (\dot{W}_t - \dot{W}_c) \quad (12)$$

The simulation for the small scale power generation system described was divided in two different stages. First, a parametric analysis on the effects of evaporative air cooling on the cycle thermal efficiency, net power generation and specific fuel consumption was done, comparing the GMTC and GMTEC cycles for an ambient temperature ranging from 10 to 50 °C with an air relative humidity of 5%. Then, in a second stage, another simulation was carried out using annual weather data from the TRY for Brasília, as an input for hourly ambient air conditions. Thus the efficiency curves for thermal efficiency and specific fuel consumption for both cycles for a whole year of operation were compared.

**4.2 Case 2 - Cooling Load in the Community Center of the University of Brasília**

In order to simulate the heat exchanges between the UnB Community Center canvas and its surroundings a meshing of the canvas surface was done by means of a network of small triangular plane elements, as shown at Fig. 6a. The rendering process has result in a non uniform mesh of 1914 triangles as shown in Fig. 6b, where each individual triangle has its space coordinates defined. A numerical simulation procedure was then applied, based in the calculation of hourly values of direct, diffuse and total solar irradiation for each isolated triangle in the grid, using equations available for solar irradiation computation (MCQUISTON and SPITLER, 1994) adjusted for condition at the latitude (15°52' South) and longitude (47°55') of Brasília.

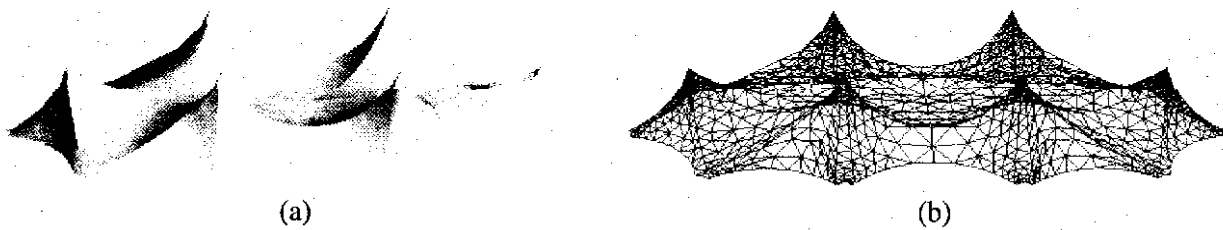


**Figure 6 -** Computer modeling of the UnB Community Center canvas (a), with its triangular elements based mesh resulting from the numeric rendering process (b).

In order to simplify the canvas heat transfer analysis the following assumptions were made: (1) steady state heat transfer regime, (2) negligible thermal capacity of the canvas material; (3) outside forced convective conditions on the canvas approximated by the horizontal flat plate case; (4) free convective conditions bellow the canvas surface are approximated by the horizontal bottom surface of a hot plate case; (5) radiant heat transfer between each internal surface element of the canvas and the floor is treated as exchange between a small area object and a large isothermal surface (6) inside air bellow the canvas is assumed a non-participating media. On the basis of these assumptions Fig. 7 shows energy flows for a generic canvas surface element.

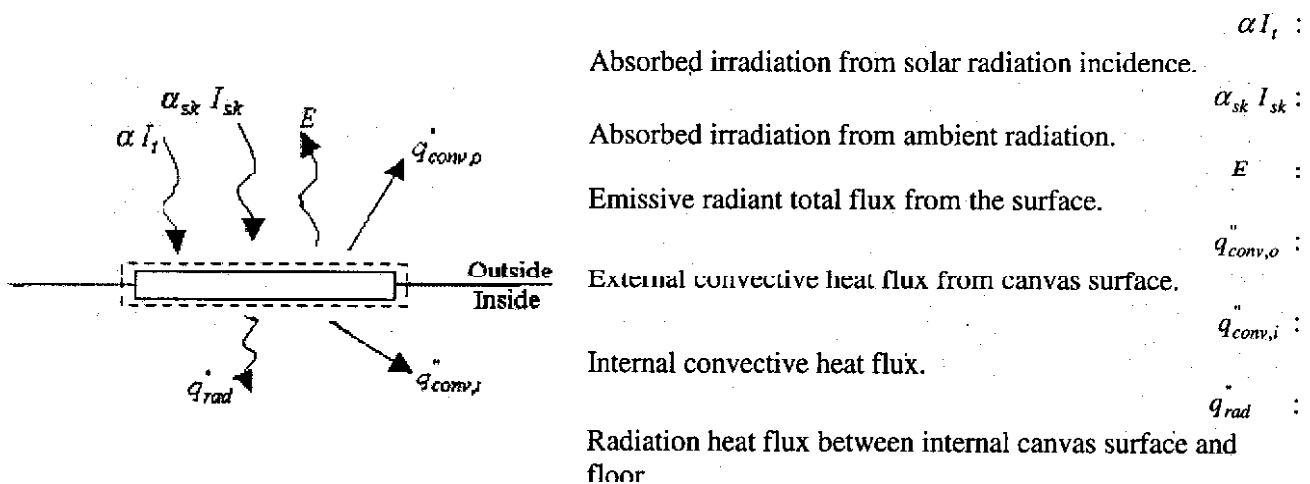


**Figure 7 -** Energy balance for an isolated triangular element in the canvas surface.

A application of the energy conservation principle to each canvas surface element is them written as follows,

$$\alpha I_t + \alpha_{sk} I_{sk} - E - q_{conv,o}'' - q_{conv,i}'' - q_{rad}'' = 0 \quad (13)$$

where  $\alpha$  and  $\alpha_{sk}$  are the total hemispheric absorptivity of the canvas outside surface to solar radiation and sky ambient radiation spectrum respectively, which are taken as having both a value of 0.15. In this energy balance equation the ambient irradiation from sky is defined by (INCROPERA and DEWITT, 1998):

$$I_{sk} = \sigma T_{sk}^4 \quad (14)$$

while radiation emission from canvas external surface is given by,

$$E = \varepsilon \sigma T_{su}^4 \quad (15)$$

where  $\varepsilon$  is the canvas surface emissivity (about 0.1) and  $\sigma$  is the Stefan-Boltzmann constant ( $5.67 \times 10^{-8} \text{ W/m}^2\text{K}^4$ ).

On the internal side of the canvas, a free convection heat transfer condition is assumed which is associated with a heat flux given by,

$$q_{conv,o}'' = \bar{h}_o \cdot (T_{su} - T_o) \quad (16)$$

and

$$q_{conv,i}'' = \bar{h}_i \cdot (T_{su} - T_i) \quad (17)$$

where  $T_o$  and  $T_i$  are the outside and inside dry bulb air temperatures respectively. On the basis of the TRY weather data for Brasília, available data for simulation presents a dry bulb outside temperature between 10 and 35 °C with air velocities ranging from 0 to 15m/s. which implies in a laminar flow condition outside the canvas surface.

Taking into account assumptions "3" and "4", and adopting a simplified approach for heat transfer analysis, average heat transfer coefficients for internal and external convective heat exchanges  $\bar{h}_o$  and  $\bar{h}_i$  are obtained from the following empirical correlations (INCROPERA and DEWITT, 1998):

$$\bar{h}_o = 0,664 \cdot L_c^{-1} \cdot k_o \cdot \text{Re}^{1/2} \cdot \text{Pr}^{1/3} \quad (\text{Pr} \geq 0,6) \quad (18)$$

and

$$\bar{h}_i = 0,27 \cdot (w/2)^{-1} \cdot k_i \cdot \text{Ra}_L^{1/4} \quad (10^5 \leq \text{Ra}_L \leq 10^{10}) \quad (19)$$

where  $L_c$  and  $w$  are the length and width of each triangular surface element of the canvas, respectively, with  $\text{Re}$ ,  $\text{Pr}$  and  $\text{Ra}_L$  the Reynolds, Prandtl and Rayleigh numbers.

Heat transfer by radiation between the inferior the canvas surface and the UnB Community Center floor is (with the assumption "5") given by (INCROPERA and DEWITT 1998),

$$q_{rad}'' = \varepsilon \cdot \sigma \cdot (T_{su}^4 - T_f^4) \quad (20)$$

where  $T_f$  is the floor temperature which is assumed as having the same value of the ambient air temperature. Introducing Eqs.(13-16;19) into Eq. (12), after some manipulation allow to write the following equation,

$$a \cdot T_s^4 + b \cdot T_s + c = 0 \quad (21)$$

where coefficients  $a$ ,  $b$  e  $c$  are given by:  $a = 2\varepsilon\sigma$ ,  $b = \bar{h}_o + \bar{h}_i$  e  $c = -\alpha I_t - \varepsilon\sigma(T_{sk}^4 + T_f^4) - \bar{h}_o T_o - \bar{h}_i T_i$ .



Equation (21) can be solved in order to obtain the canvas surface temperature at each triangular element on the surface of the canvas, which is then introduced in Eq. (17), in order to get the internal convective heat flux to air below the element,  $\dot{q}$ . Repeating this procedure for all canvas triangular elements, allow to integrate for all the canvas surface of the UnB Community Center, by means of,

$$\dot{Q}_{Canvas} = \int_A \dot{q}'' \cdot dA \tag{22}$$

Besides this external thermal load, the internal heat gain due to occupants must also be determined. Sensible and latent heat for each seated person is taken as 75 and 55 W, respectively, (ASHRAE, 1989). Since the UnB Community Center capacity is for about 3000 seated occupants, the total sensible and latent heat internal heat loads are of 225 and 165 kW respectively. Other internal heat sources are not considered.

A computational application of the above equations, together with the consideration of internal heat gain due to occupants, allow to simulate the Community Center cooling load, as well as the performance of the evaporative cooling direct spraying system. The simulations were carried out for TRY data at Brasilia in March, 21 summer day.

## 5 Case Studies – Results and Discussion

### 5.1 Case 1 - Air Evaporative Cooling for Microturbine Based Power Cycle

Figures 8a and 8b shows changes in thermal efficiency and net power output of the microturbine cycle as a function of ambient air temperature variation for both the GMTC and EGMTC cycles. As ambient air temperature increases compressor power consumption will also increase and it can be easily seen that this results in a reduction in net power output from the cycle as well as thermal efficiency will also decrease. However the cycle without evaporative air cooling at compressor supply (GMTC) has a greater sensibility to ambient air temperature increase, i.e., net power production and cycle efficiency losses are higher without air evaporative cooling for the same ambient air temperature increase. This is due to the fact that as ambient air temperature increase, the difference between dry and wet bulb air temperatures will also increase resulting in a more efficient evaporative air cooling process. Figure 8a also shows that the use of evaporative cooling at the compressor supply can increase net power production from the microturbine cycle up to 2 %, which allow a reduction in specific fuel consumption about 4.3% for the operating conditions considered.

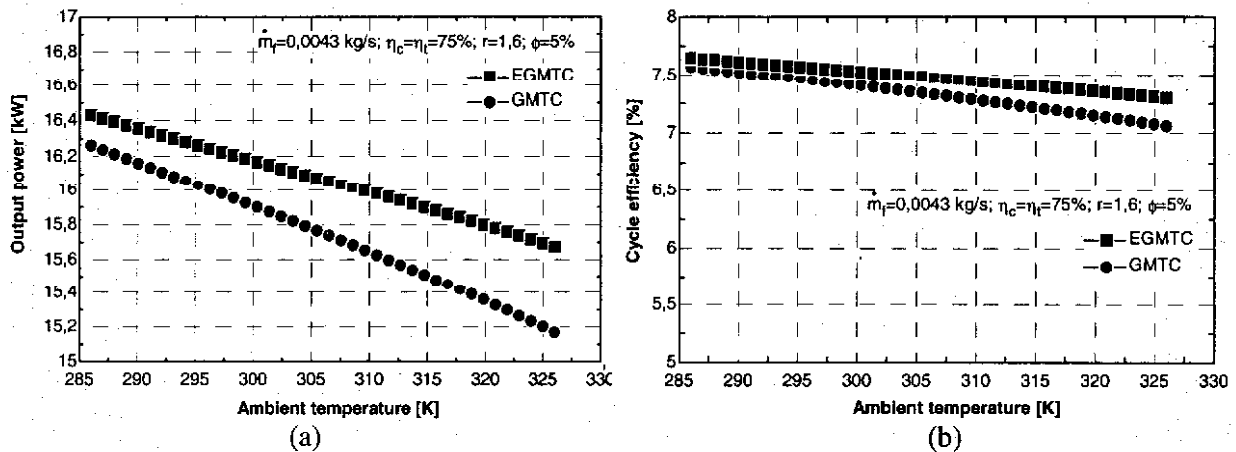


Figure 8 - Net power output (a) and cycle thermal efficiency (b) as a function of ambient air temperature for GMTC (without evaporative cooling) and EGMTC (with evaporative cooling).

Figure 9a shows the thermal efficiency hourly changes for both GMTEC and GMTCC cycles during whole year of operation based in TRY data for Brasilia. It can be seen that the use of an evaporative panel at compressor supply does not change significantly the thermal efficiency which was about 7.3 % along the whole year. On the other hand, a small reduction in fuel specific consumption about 1.5 % can be observed from Fig. 9b,

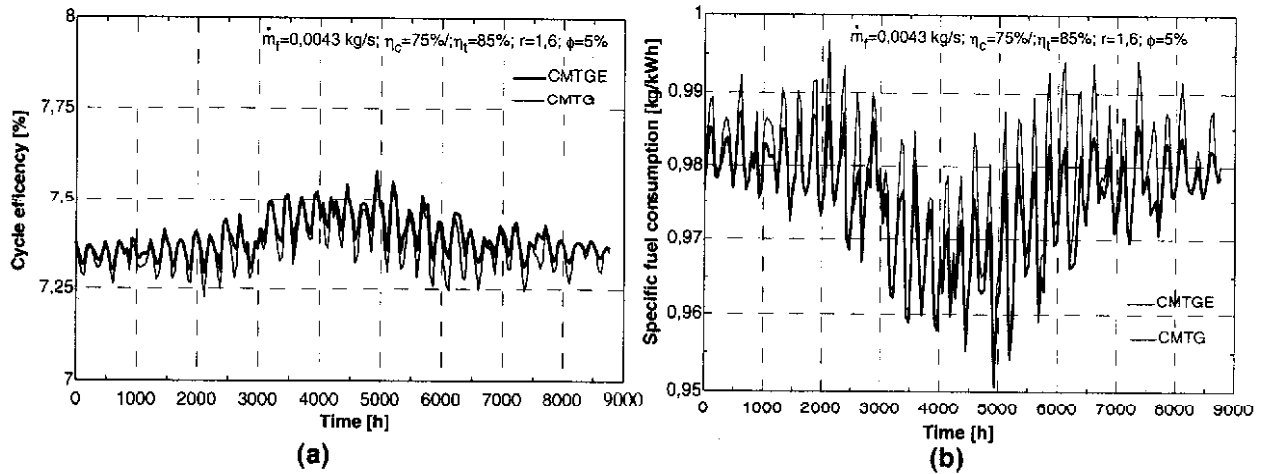


Figure 9 - Annual change in thermal efficiency (a) and specific fuel consumption (b) for both the GMTEC and GMTC cycles.

### 5.2 Case 2 – Cooling Load in the Community Center of the University of Brasília

Figure 10 shows the daily changes in direct, diffuse and total irradiation computed for the full canvas surface of the UnB Community Center after numeric integration for March, 21 of the TRY for Brasília. As expected, irradiation on the exterior canvas surface is higher about noon.

According with the previous model presented for heat transfer at each canvas surface element, the average canvas surface temperature was also calculated for this simulation case and results in a maximum value about 57 °C. Such condition is related with a maximum heat transfer rate form canvas inferior surface and the floor surface below it about 25 kW at 12:00 h. The total cooling load for space conditioning purposes is given by the sum of heat gain from the canvas and internal load due to occupants and attains for this simulation case study a maximum value about 415 kW.

For the peak cooling load obtained from simulation, a water flow rate to be sprayed in the ambient about 608 kg/h was calculated by considering the latent enthalpy of water. This requires a spraying network with 150 spray nozzles and a centrifugal pump of 3.73 kW (5 HP) with a working pressure of 800 PSI. (Prime Tech™).

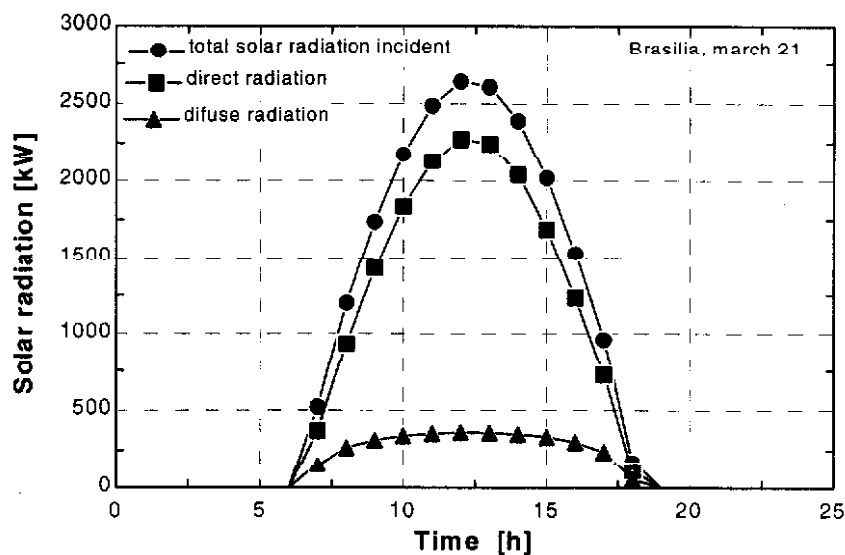


Figure 10 - Daily change in diffuse, direct and total radiation for the whole canvas surface.

## 6 Conclusions

### 6.1 Case 1 – Air Evaporative Cooling for Microturbine Based Power Cycle

Application of an evaporative direct cooling system to air conditioning at compressor supply in a microturbine power generation cycle has show a significant potential for efficiency improvement and should be further investigated, particularly with respect to its influences on combustion process and emissions. In the parametric analysis carried out, the effects of evaporative air conditioning at the inlet of an open Brayton microturbine based cycle has been analyzed. It was verified that the more ambient conditions are worst the more effective the evaporative cooling system will be in cycle efficiency improvement. For the operating conditions considered the GMTEC and GMTC cycles has present similar results but, increase in thermal efficiency was about 2% with fuel savings around 4.5% for the EGMTC case.

In the simulation for annual operation at TRY weather conditions for Brasília using the same operating data from the parametric analysis, the thermal efficiencies of both the GMTEC and GMTC cycles has been almost the same. A possible explanation to this fact is related with the fact that as power consumption at the compressor is reduced thanks to the evaporative cooling system a similar reduction in microturbine power output will occur, since heat added to combustion chamber was fixed by a constant fuel flow rate.

### 6.2 Case 2 – Cooling Load in the Community Center of the University of Brasília

A cooling load analysis for the canvas surface of a community center was presented with the goal of sizing a direct spraying system for thermal comfort. An energy balance for individual surface elements obtained from a rendering technique applied to the canvas was proposed for global cooling load integration.

The resulting sensible and latent gain affecting the global cooling load were computed showing that the sensible load can represent about 6 % of the total cooling load. On the other hand, the total cooling load calculated of 415 kW requires about 150 sprays. This number of sprays is almost 50 % small than the existing number which suggests an inadequate sizing of the present system due to an underestimated cooling load. As a matter of fact some complaints from occupants with respect to an uncomfortable ambient had been reported. This support a hypothesis that the existing installation was based in a rough estimation of the peak cooling load. Then the proposed method of cooling load calculation seems to be adequate for the direct spraying system sizing.

However some improvements in the proposed technique are still necessary. For instance, the influence of the slope of each individual element on the convective heat transfer bellow the canvas should be considered. Besides, a modeling of heat and mass transfer from the water drops formed after spraying in the ambient air, might give us a better evaluation of the required water mass flow rate. These aspects will be better considered in further studies on this theme.

## References

- ASHRAE. *Ashrae handbook fundamentals-SI*. Atlanta: American Society of Heating, Refrigerating and Air Conditioning Engineers, 1989.
- BASSIY, A. M. Effects of evaporative inlet and aftercooling on the recuperated gas turbine cycle. *Applied Thermal Engineering*, Oxford, v. 21, p. 1875-1890, May 2001.
- CAMARGO, J. R.; EBINUMA, C. D. Resfriamento evaporativo: poupando a energia e o meio ambiente. In: JORNADA DE INICIAÇÃO CIENTÍFICA E DE PÓS-GRADUAÇÃO, 2001, São Paulo. *Anais...* São Paulo: UNESP/FEG, 2001. 1 CD-ROM.
- COHEN, H.; ROGERS, G. F. C.; SARAVANAMUTTOO, H. I. H. *Gas turbine theory*. London: Longman, 1996. 414p.
- DE LUCIA, M.; LANFRANCHI, C.; BOGGIO, V. Benefits of compressor inlet air cooling for gas turbine cogeneration plants. In: INTERNATIONAL GAS TURBINE AND AEROENGINE CONGRESS AN EXPOSITION, 1995, Houston. *Proceedings...* Houston: ASME, 1995. 1 CD-ROM.
- DE LUCIA, M. et al. Benefits of compressor inlet air cooling for gas turbine cogeneration plants. In: INTERNATIONAL GAS TURBINE AND AEROENGINE CONGRESS AN EXPOSITION, 1997, Orlando. *Proceedings...* Orlando: ASME, 1997. 1 CD-ROM.

- GUIMARÃES, E. T. *A new approach to turbine inlet air cooling*. Rio de Janeiro: Turbine Inlet Cooling System, 2000.
- INCROPERA, F. P.; DEWITT, D. P. *Fundamentals of heat and mass transfer*. Rio de Janeiro: LTC, 1998.
- JOUDI, K. A., MEHDI, S. M. Application of indirect evaporative cooling to variable domestic cooling load. *Energy Conversion and Management*. London, v. 41, p. 1931-1951, Dec. 2000.
- MCQUISTON, F. C.; SPITLER, J. D. *Cooling and heating load calculation manual*. Atlanta: American Society of Heating, Refrigerating and Air-Conditioning Engineers, 1994.
- SANTOS, F. A. *Projeto e estudo de desempenho de uma microturbina multicomcombustível*. 2002. 40f. Trabalho de conclusão de Curso (Graduação) - Faculdade de Tecnologia. Universidade de Brasília. Brasília, 2002.
- WATT, J. *Evaporative air conditioning handbook*. New York: Routledge, Chapman and Hall, 1984.

## ABOUT THE AUTHORS

### Wagner Pereira de Castro

Engenheiro Mecânico pela Faculdade de Tecnologia da Universidade de Brasília, em 2003. Atualmente cursando o programa de Mestrado em Ciências Mecânicas do Departamento de Engenharia Mecânica da Universidade de Brasília.

### João Manoel Dias Pimenta

Engenheiro Mecânico pela Fundação Técnico-Educacional Souza Marques em 1988, M.Sc. em Engenharia Mecânica pela Universidade Federal de Uberlândia em 1992, Doutor em Ciências Aplicadas pelo Laboratoire de Thermodynamique da Université de Liège em 1997. Atualmente ocupa o posto de professor adjunto do Departamento de Engenharia Mecânica da Universidade de Brasília, onde atua em nível de graduação e pós-graduação.